Enhanced sensitivity of MoSe2 monolayer for gas adsorption induced by electric field

Ai, W.; Kou, L.; Hu, X.; Wang, Y.; Krasheninnikov, A.; Sun, L.; Shen, X.;

Originally published:

August 2019

Journal of Physics: Condensed Matter 31(2019), 445301

DOI: https://doi.org/10.1088/1361-648X/ab29d8

Enhanced Sensitivity of $MoSe_2$ Monolayer for Gas Adsorption Induced by Electric Field

Wen Ai,[1] Liangzhi Kou,[3] Xiaohui Hu,[*1,2] Yifeng Wang,[1,2] Arkady V. Krasheninnikov,[4,5] Litao Sun,[6] Xiaodong Shen[1,2]

[1] College of Materials Science and Engineering, Nanjing Tech University, Nanjing 211816, China

[2] Jiangsu Collaborative Innovation Center for Advanced Inorganic Function Composites, Nanjing Tech University, Nanjing 211816, China

[3] School of Chemistry, Physics and Mechanical Engineering Faculty, Queensland University of Technology, Garden Point Campus, Brisbane, QLD 4001, Australia

[4] Institute of Ion Beam Physics and Materials Research, Helmholtz-Zentrum Dresden-Rossendorf, 01314 Dresden, Germany

[5] Department of Applied Physics, Aalto University School of Science, PO Box 11100, 00076 Aalto, Finland

[6] SEU-FEI Nano-Pico Center, Key Laboratory of MEMS of Ministry of Education, Collaborative Innovation Center for Micro/Nano Fabrication, Device and System, Southeast University, Nanjing 210096, China

Corresponding Author: xiaohui.hu@njtech.edu.cn (XH)

Abstract

According to recent studies, gas sensors based on $MoSe_2$ have better detection performance than graphene-based sensors, especially for N-based gas molecules, but the reason for that is not fully understood at the microscopic level. Here, we investigate the adsorption of CO, CO_2, NH_3, NO and NO_2 gas molecules on $MoSe_2$ monolayer by the density functional theory calculations. Our results reveal that indeed $MoSe_2$ monolayer is more sensitive to adsorption of N-containing gas molecules than C-containing, which can be attributed to the distinct charge transfer between the gas molecules and $MoSe_2$. The conductance was further calculated using the nonequilibrium Green's function (NEGF) formalism. The reduced conductance was found for NH_3 and NO_2 adsorbed $MoSe_2$, consistent with the high sensitivity of $MoSe_2$ for NH_3 and NO_2 molecules in the recent experiments. In addition, the adsorption sensitivity can significantly be improved by an external electric field, which implies the controllable gas detection by $MoSe_2$. The magnetic moments of adsorbed NO and NO_2 molecules can also be effectively modulated by the field-sensitive charge transfer. Our results not only give microscopic explanations to the recent experiments, but also suggest using $MoSe_2$ as a promising material for controlled gas sensing.

Keywords: transition metal dichalcogenides, gas sensor, density functional theory calculations, electric field

Introduction

Two-dimensional (2D) nanomaterials are ideal platforms for building nanoscale sensors due to their reduced dimensionality and excellent properties [1-8]. Recently,

2D transition metal dichalcogenides (TMDs) have attracted great interest as chemical sensors owing to their high carrier mobility [9-14], large surface-to-volume ratio [15-21], and rapid electrical response to the changes in the environments [22-24]. For instance, monolayer and multi-layer MoS_2 films have been found to be extremely sensitive to the environmental gas molecules, especially to NO, NO_2 and NH_3 [25-27]. $MoSe_2$ layer, one of the most important materials in the family of 2D TMDs, is expected to have excellent sensing performance due to similar electronic properties, and also the fact that the phototransistors based on $MoSe_2$ exhibited outstanding responsivity, high specific detectivity and fast response time [28, 29]. Indeed, recent experimental studies demonstrated that $MoSe_2$ sheets possess a competitive advantage over traditional graphene sensors [30]. In addition, Late *et al.* reported high-performance $MoSe_2$-based NH_3 gas sensors with a detection limit down to 50 ppm [31]. More recently, a multilayer $MoSe_2$ gas sensor has exhibited ultra-high sensitivity ($S \sim 2\times10^3$ for NO_2 at 300 ppm), owing to changes of the gap states near the valence band induced by the NO_2 adsorption [32]. However, the formation of these gap states has not been explained, and further verification is desired to carry out. These reports have stimulated exploration of $MoSe_2$ as a prospective sensing material.

In fact, the adsorption performance is mainly based on the charge transfer between the adsorption substrate and the gas molecules, which plays an important role in determining the performance of gas sensors. Therefore, effective control for electron transfer between gas molecules and sensing materials can modulate the sensitivity.

Calculations have demonstrated that the sensing properties of low dimensional materials, such as carbon nanotubes [33, 34], graphene [35, 36] and MoS_2 [37], are controllable by external electric field. For example, recent studies indicated that the adsorption of NO_2 based on Ga-doped graphene was effectively enhanced by the electric field, as manifested by the increase in adsorption energy [36]. Moreover, the charge transfer between the adsorbed molecule and MoS_2 can also be controlled by the external electric field [37]. In addition, the applied electric field could significantly enhance the CO gas sensitivity of the antimonene [38], which is beneficial for the application of CO gas sensor at room temperature. These studies suggested that the external electric field can dramatically change the affinity and electronic properties of the adsorption system. Therefore, it is expected that the electric field can effectively modulate the charge transfer between gas molecules and $MoSe_2$, which inspired us to study if sensitivity of $MoSe_2$ for gas sensors can be improved by applying external electric field.

In this work, by means of systematic density functional theory (DFT) calculations, we examine the most stable adsorption configurations and also evaluate adsorption energy, charge transfer, and magnetic properties of gas molecules (CO, CO_2, NH_3, NO and NO_2) on $MoSe_2$ monolayer. The results show that the adsorption energies of N-based gas molecules are larger than those for CO and CO_2 adsorption, which is related to the distinct charge transfer between the gas molecules and $MoSe_2$. The reduced conductance was found for NH_3, NO and NO_2 adsorbed $MoSe_2$, which well explains

the high sensitivity of $MoSe_2$ to NH_3 and NO_2 adsorption as seen in recent experiments. In addition, the adsorption sensitivity can be significantly improved by an external electric field. The magnetic moments of adsorbed NO and NO_2 molecules can effectively be modulated by the charge transfer, which is sensitive to the applied electric field. Our results not only explain the recent experiments [31] at the atomistic level, but also suggest using $MoSe_2$ as a superior gas sensor.

Calculation details

Our calculations were carried out using the VASP package [39, 40] based on DFT. The generalized gradient approximation (GGA) with the Perdew-Burke-Ernzerhof (PBE) functional was used for the exchange and correlation interactions [41]. The projector-augmented-wave (PAW) method was employed to describe electron-ion interactions [42, 43]. Van der Waals corrections were included through Grimme's DFT-D2 method as implemented in VASP [44, 45]. The plane wave cutoff energy was set to 500 eV, because a higher value had little effect on the results. The structures were relaxed until the energy and the force on each atom were less than 10^{-5} eV and 0.01 eV/Å, respectively. A k-point sampling of 9 × 9 × 1 and 19 × 19 × 1 were used for the structural relaxations and self-consistent calculations. The vacuum region of 15 Å was introduced to avoid interaction between periodic images of slabs. The charge transfer between gas molecules and $MoSe_2$ was calculated using Bader analysis [46]. Spin polarization was included in the calculations of the adsorption of paramagnetic molecules NO and NO_2. The electronic transport properties were studied by the NEGF

method implemented in the TRANSIESTA package [47].

Results and discussion

To model the absorption of CO, CO_2, NH_3, NO and NO_2 molecules on the surface of $MoSe_2$ monolayer, a 4 × 4 supercell of $MoSe_2$ was chosen. The optimized lattice constant of $MoSe_2$ monolayer was found to be 3.32 Å, consistent with the previous results [48,49]. In order to obtain the most stable adsorption configuration, the four different adsorption sites were considered (see Figure S1 in Supporting Information). (i) H site (on the top of a hexagon center), (ii) Tm (on the top of a Mo atom), (iii) Ts (on the top of a Se atom), (iv) B site (on the top of a Mo-Se bond). The top and side views of the most favorable configurations for CO, CO_2, NH_3, NO and NO_2 adsorbed on $MoSe_2$ are shown in Figure 1. For the CO and CO_2 molecules, the C atom is located at the Tm and Ts sites. The adsorption distance between the CO molecule and $MoSe_2$ (2.94 Å) is smaller than the value for CO_2 adsorption (3.30 Å). However, NH_3 and NO_2 molecules are located at the H site. The distances for NH_3 and NO_2 adsorption are 2.72 Å and 2.77 Å, respectively. In contrast, for NO, the molecule moves to the B site with the adsorption distance of 2.88 Å, as shown in Figure 2(a). The values indicate that upon adsorption the N-based gas molecules have the smaller distance as compared to those for CO and CO_2 molecules.

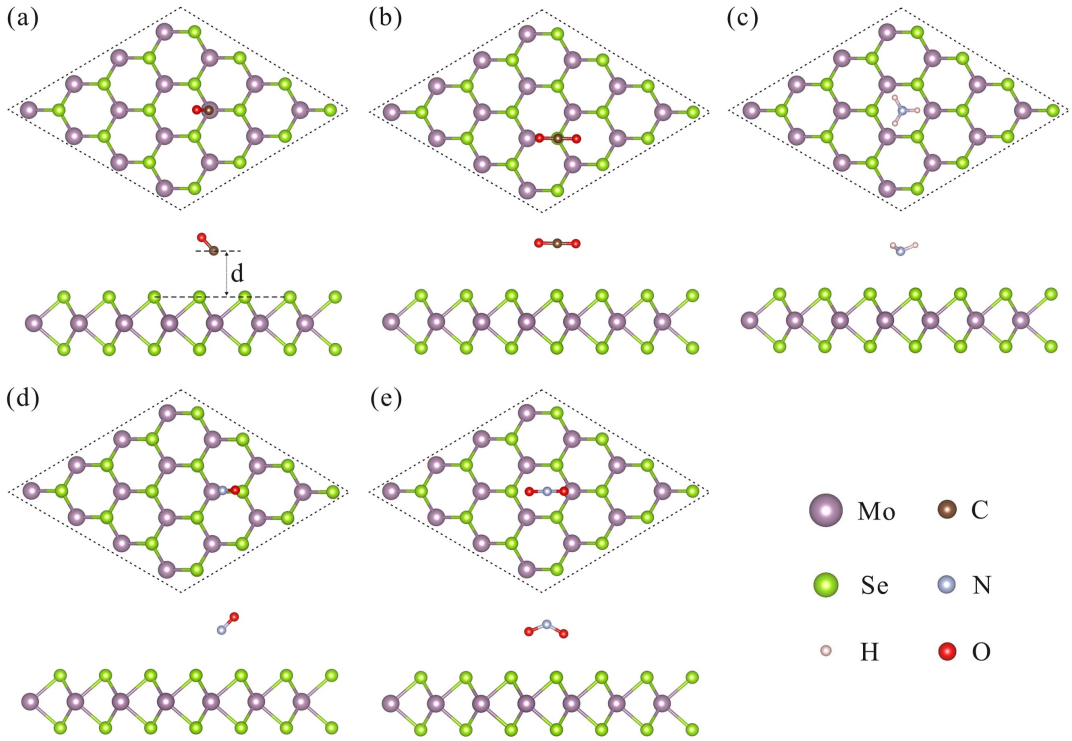

Figure 1. Top and side views of (a-e) the most favorable configurations of (a) CO, (b) CO_2, (c) NH_3, (d) NO, and (e) NO_2 adsorbed on $MoSe_2$ monolayer. The definition for the adsorption distance d is given in (a).

In order to get a quantitative description of the adsorption strength on $MoSe_2$ monolayer for different gas molecules, the adsorption energy was computed. The adsorption energy is defined as $E_a = E_{MoSe_2} + E_{molecule} - E_{total}$, where E_{total} is the total energy of $MoSe_2$ with an absorbed molecule, E_{MoSe_2} and $E_{molecule}$ are the total energies of the pristine $MoSe_2$ and isolated molecule, respectively. According to this definition, a more positive E_a value indicates a stronger adsorption. The calculated values of adsorption energy are displayed in Figure 2b. It is found that CO has the minimum adsorption energy of 0.099 eV, while NO_2 has the maximum adsorption energy of 0.199 eV. The adsorption energies of CO_2, NO, and NH_3 are 0.144, 0.167,

and 0.187eV, respectively. The results show that the adsorption energies of N-based gases are larger than those for CO and CO_2 adsorption, which well correlates with the adsorption distances presented in Figure 2a. This indicates that $MoSe_2$ is more sensitive to adsorption of N-based gases, which is similar to MoS_2 and graphene that are sensitive to adsorption of N-based gases [14,26]. Among them, NH_3 and NO_2 have the highest adsorption energy, which explains the higher sensitivity to NH_3 and NO_2 adsorption on $MoSe_2$ as seen in the recent experiments [31, 32].

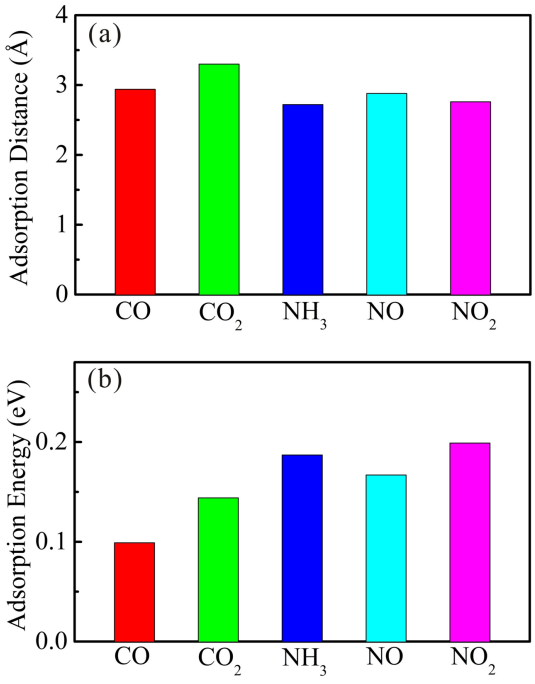

Figure 2. (a) Distance between the gas molecule and the $MoSe_2$ monolayer, defined as in Figure 1a. (b) Adsorption energy for CO, CO_2, NH_3, NO, and NO_2 on $MoSe_2$ monolayer.

Previous studies indicate that charge transfer plays an important role in the adsorption strength and the decrease in the resistance of MoS_2 [50]. Thus, we calculated the charge difference between the gas molecules and $MoSe_2$ monolayer (Figure 3), which is defined as $\Delta\rho = \rho_{gas/MoSe_2} - \rho_{gas} - \rho_{MoSe_2}$, where $\rho_{gas/MoSe_2}$, ρ_{gas} and

ρ_{MoSe_2} represent the charge density of the gas molecules adsorption system, the isolated gas molecule and the free $MoSe_2$ monolayer, respectively. Both the gas molecule and free $MoSe_2$ have the same coordination as that in the adsorbed configuration. To have a quantitative picture, Bader analysis was performed to extract the charge transfer amount induced by the gas adsorption. As shown in Figure 3a and 3b, for CO and CO_2 adsorption, the small amount of charge transfer (0.015 e and 0.025 e, respectively) is observed from $MoSe_2$ monolayer to the gas molecules, indicating the weak binding. However, for N-based gas molecules, larger charge transfer takes place, suggesting a stronger binding between the gas molecules and $MoSe_2$ monolayer. Especially for NO_2, up to 0.149 e is transferred from $MoSe_2$ monolayer to the molecule (Figure 3e), which has the strongest binding. For NH_3 and NO adsorption in Figure 3c and d, the charge transfer (0.029 e and 0.035 e, respectively) is smaller than that for NO_2, but still larger than those for CO and CO_2. The comparison of the amount of the charge transfer and the adsorption energy (strength) presented in Figure 2b shows a clear correlation, which can help us to understand the mechanism for gas molecule adsorption on $MoSe_2$ monolayer. In addition, it is evident from Figure 3 that most molecules (such as CO, CO_2, NO and NO_2) are charge acceptors, whereas NH_3 behaves as a charge donor. The phenomenon is similar to the cases of gas adsorption on graphene and MoS_2 [37,51], where the gas molecules also behave as either charge acceptors or donors. For the n-type $MoSe_2$, some electrons have already existed in the conduction band. Upon CO, CO_2, NO and NO_2 adsorption, electron charge is transferred to the gas molecules from

$MoSe_2$, leading to an increased resistance and decreased current of $MoSe_2$. Then, the mechanism of the $MoSe_2$-FET gas sensor for NO_2 can be understood [32].

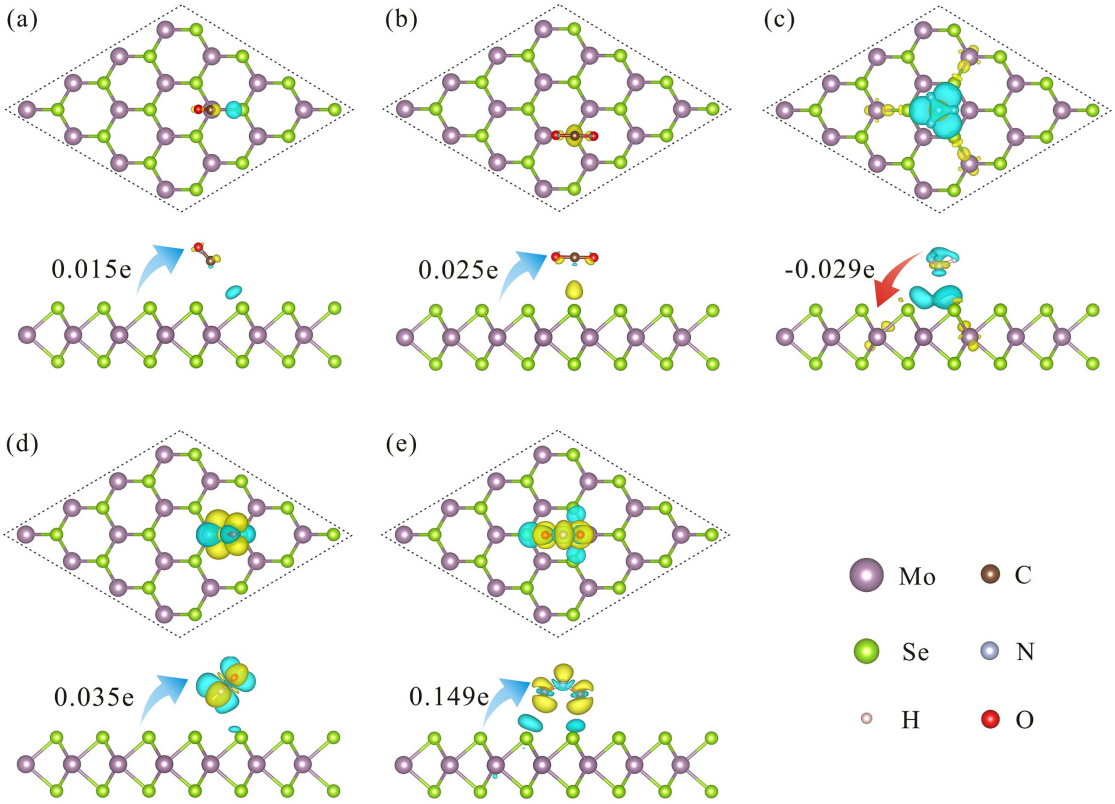

Figure 3. The charge difference between $MoSe_2$ monolayer and gas molecules for (a) CO, (b) CO_2, (c) NH_3, (d) NO and (e) NO_2. The isosurface is taken at 6.0×10^{-4} e/Å^3. The electron accumulation (depletion) is indicated by yellow (blue) color. The direction (indicated by an arrow) and value of the charge transfer are shown.

Next, we examine the effects of gas adsorption on the electronic properties of $MoSe_2$ monolayer. Figure 4a shows the band structure of $MoSe_2$ monolayer, which has a direct bandgap of 1.44 eV, in accordance with previous reported results [48,49]. Figure 4b-d present the band structure of $MoSe_2$ monolayer with the adsorption of CO, CO_2 and NH_3, as well as the projected band structure from the gas molecules. It is found that upon CO, CO_2 and NH_3 adsorption, neither the valence bands nor conduction band of

$MoSe_2$ monolayer is significantly influenced, as the impurity states induced by gas molecules located away from the Fermi level. Thus, CO, CO_2 and NH_3 adsorption does not modify the band structure near the Fermi level, and has no substantial influence on the electronic structure of $MoSe_2$ monolayer. On the other hand, the spin-polarized band structure of NO and NO_2 adsorbed $MoSe_2$ is displayed in Figure 4e and f. It is seen that for paramagnetic NO and NO_2 adsorption, some flat impurity states are clearly observed in the band gap of the host $MoSe_2$ monolayer. Specifically, NO introduces two spin-up states at -0.12, 0.12 eV and one spin-down state at 0.55 eV close to the Fermi level in the band gap (see Figure 4e). NO_2 introduces one spin-down state at 0.14 eV above the Fermi level in the band gap, given in Figure 4f. Our findings clearly explain the origin of the gap states in NO_2 adsorbed $MoSe_2$ in the recent experiments [32].

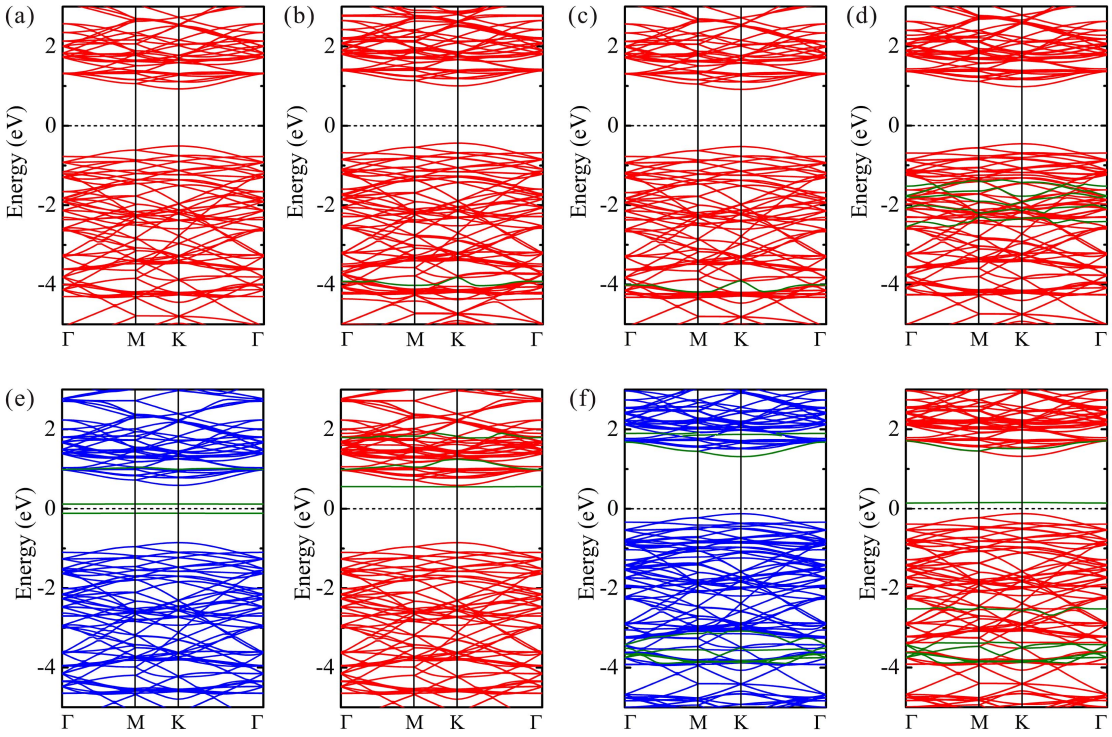

Figure 4. (a) The band structure of pristine $MoSe_2$. Band structure of (b) CO, (c) CO_2, (d) NH_3, (e) NO and (f) NO_2 adsorbed on $MoSe_2$ monolayer. The blue and red lines denote spin-up and spin-

down channels, respectively. The olive lines represent the projected band structure of the adsorbed gas molecules.

To further analyze the changes in electronic structure of $MoSe_2$ upon adsorption of the gas molecules, the projected density of states (PDOS) are calculated and presented in Figure 5. In the pristine $MoSe_2$ monolayer, the conduction band minimum is mainly described by Mo d_{z^2} orbitals, while the valence band maximum is mostly contributed from Mo d_{xy} and d_{x^2} orbitals [48, 49]. For the CO and CO_2 adsorption, we did not observe noticeable changes around the Fermi level upon adsorption of the molecules, as indicated in Figure 5b and c, which is consistent with their small adsorption energies. Meanwhile, the adsorption of the NH_3 molecule induces some impurity states in the energy range around -2 eV, which leads to the hybridization of the N p_z orbital with the d_{z^2}, d_{x^2} and d_{xy} orbitals of the Mo atom. Overall, the adsorption of CO, CO_2 and NH_3 molecules does not have a noticeable effect on the DOS near the Fermi level. For the adsorption of NO, it can be seen from Figure 5e that the NO p_y and p_z orbitals dominate two DOS peaks around the Fermi level, which results in the flat impurity states for the spin-up electrons (see Figure 4e). Similarly, the adsorption of NO_2 produces a spin-down impurity state near the Fermi level, which is mainly composed of O p_z orbitals, as shown in Figure 5f. It can be concluded that the adsorption of paramagnetic molecules NO and NO_2 induces the impurity states around the Fermi level, which have the obvious influence on the electronic structure of $MoSe_2$, as manifested in their higher adsorption energy.

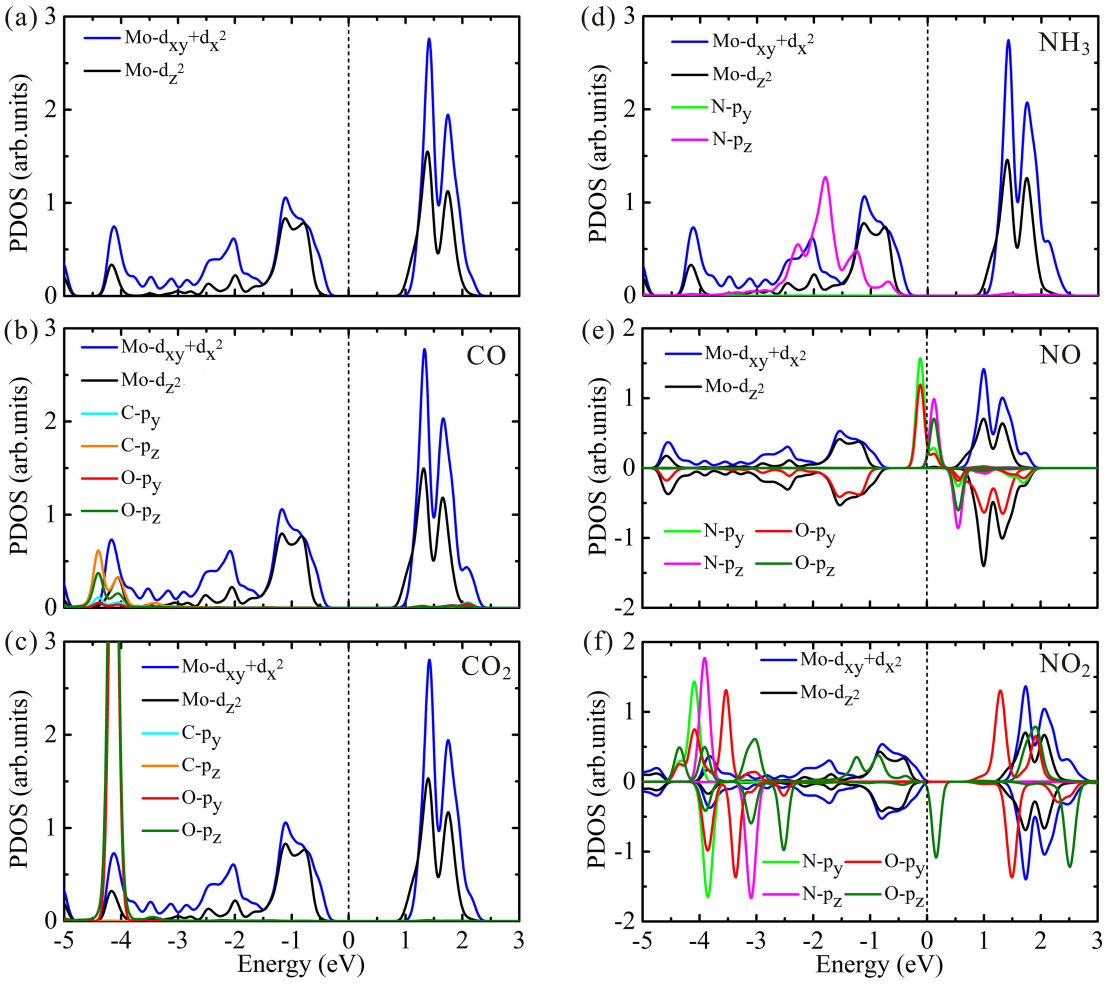

Figure 5. (a) PDOS of pristine $MoSe_2$. PDOS of (b) CO, (c) CO_2, (d) NH_3, (e) NO and (f) NO_2 adsorbed on $MoSe_2$ monolayer.

Although the electronic properties of $MoSe_2$ are not significantly influenced by CO, CO_2, and NH_3 adsorption, the resistivity of the system can be directly measured experimentally, which can be used as a signal for detecting gas molecules. In order to explore the resistivity change, we carried out the calculation of the conductance for $MoSe_2$ before and after the gas adsorption by the NEGF method. A two-probe system, where semi-infinite left and right electrode regions are in contact with the central scattering region, is used to calculate the electron transport properties, as shown in Figure 6a. We chose a 4 × 4 surpercell without gas adsorption for each of the left and

right electrodes, whereas the center scattering region was represented by a 4 × 4 surpercell with adsorpbed gas molecules. Calculations for a 4 × 4 central scattering region without gas adsorption were also done for comparison. For the nonmagnetic gas molecules adsorption (CO_2), the conductance of the system was almost unchanged as compared to the pristine $MoSe_2$, while for CO and NH_3 the conductance was detectably reduced, as shown in Figure 6b. The smaller conductance means a reduced current, which can be directly used to compare with th experimental measurements. Similarly, a reduction in the conductance for NO and NO_2 adsorbed $MoSe_2$ is also observed, Figure 6c, indicating the high sensitivity of $MoSe_2$ sensor to N-based gas molecules. It should be noted that the significantly decreased conductance of $MoSe_2$ with adsorbed NH_3 and NO_2 molecules is consistent with the high sensitivity of $MoSe_2$ for NH_3 and NO_2 molecules reported in the recent experiments [31, 32].

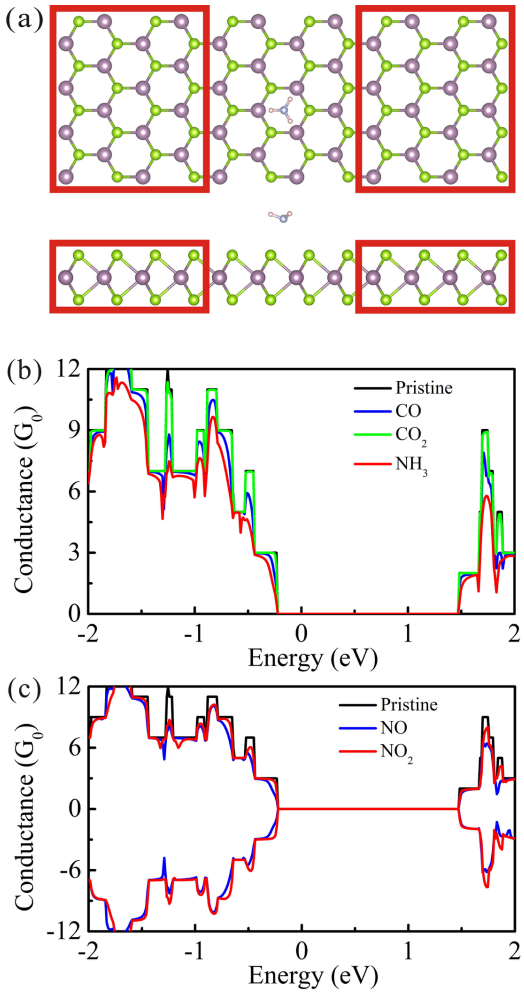

Figure 6. (a) Illustration of the two-probe systems where semi-infinite left and right electrode regions (red square region) are in contact with the central scattering region. The conductance of pristine $MoSe_2$ monolayer before and after (b) CO, CO_2 and NH_3, (c) NO, NO_2 gas molecules adsorption.

Previous studies showed that the charge transfer upon adsorption can be tuned by perpendicular electric field, which plays an important role in determining the performance of $MoSe_2$ sensor. To explore the effect of the electric field on charge transfer, we applied an external vertical electric field across the plane of $MoSe_2$ monolayer. The positive direction of the electric field is defined from $MoSe_2$ monolayer to gas molecules. Taking the paramagnetic NO and NO_2 molecules as the representative

systems, we investigated the relationship between applied electric field with charge transfer, adsorption energy, adsorption distance as well as magnetic moment, displayed in Figure 7. It can be seen from Figure 7a that the adsorption energy is sensitive to the applied electric field. Along a positive electric field, the adsorption energy consistently increases with the increasing electric field. When a negative electric field is applied, the adsorption energy gradually decreases with the increasing negative electric field. In general, higher adsorption energy implies higher sensitivity for sensing application. The adsorption energy variation can be understood from the corresponding charge transfer and the adsorption distance, displayed in Figure 7b and c. Due to the strong electronegativity of N and O atoms, NO and NO_2 molecules are negatively charged. As compared to the case without electric field, there is additional electron transferred from $MoSe_2$ to NO and NO_2 at E = 1 V/Å, which will enhance the backdonation effect, as manifested in the enhanced adsorption energy and the reduced adsorption distance. On the other hand, the electrons transfer from NO and NO_2 to $MoSe_2$ as the increasing negative electric field, which weakens the backdonation effect and leads to smaller adsorption energy and larger adsorption distance. The same trend in the adsorption energy with charge transfer in the presence of the electric field was found upon adsorption of gas molecules on Ga-doped graphene [36]. Our results suggest that the sensitivity of $MoSe_2$ with absorbed NO and NO_2 molecules can be significantly improved by applying an external vertical electric field.

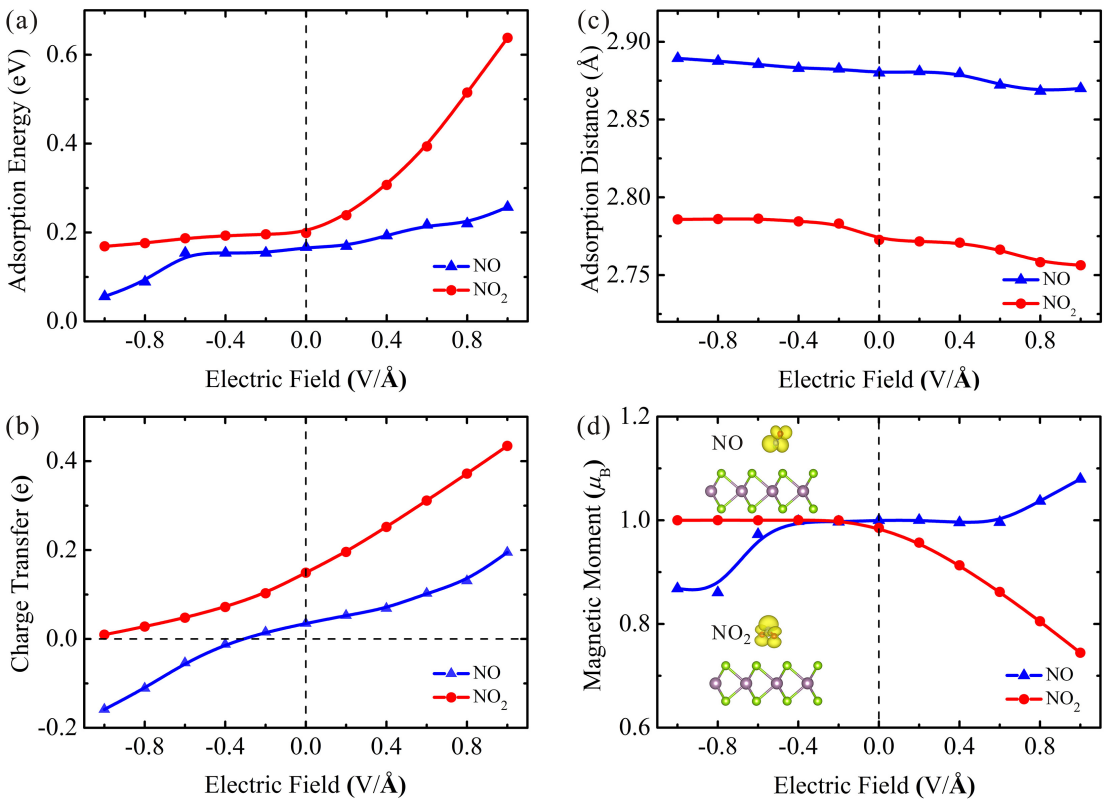

Figure 7. Variation of (a) the adsorption energy, (b) the charge transfer, (c) the adsorption distance and (d) the magnetic moment as a function of electric field strength for NO and NO_2 adsorbed on $MoSe_2$ monolayer. The insets show the spatial spin density distribution on NO and NO_2 molecules.

At the same time, the adsorption of NO and NO_2 molecules can induce a magnetic moment of 1.0 μ_B and 0.99 μ_B, respectively. The spin density distribution shown in Figure 7d indicates that the spin-polarized electrons are mainly located on the NO and NO_2 molecules. Interestingly, the magnetic moment can be tuned by the applied electric field, as shown in Figure 7d. As for NO adsorption, the magnetic moment is almost unchanged in the low electric field strength. However, the magnetic moment reaches 1.08 μ_B or reduces to 0.87 μ_B at the electric field E = 1 V/Å and -1 V/Å, which can be attributed to the charge transfer. A Bader analysis indicates that there is 0.035 e electron transferred to NO at the absence of electric field, while NO accepts 0.195 e and donates

0.159 e at E = 1 V/Å and -1 V/Å, respectively. Similarly, for NO_2 adsorption, the magnetic moment does not change too much due to charge transfer under a negative electric field, while it decreases to 0.74 μ_B at E = 1 V/Å. Thus, the magnetic moment of NO and NO_2 gas molecules on $MoSe_2$ can be effectively modulated by applying an external vertical electric field, which provides new strategy for constructing $MoSe_2$-based spin devices.

Conclusions

In summary, using systematic DFT calculations, we have investigated the adsorption energy, charge transfer, electronic and magnetic properties of the gas molecules (CO, CO_2, NH_3, NO and NO_2) adsorbed on $MoSe_2$ monolayer. The results show that the adsorption energies of N-based gas molecules are larger than those for CO and CO_2 molecules, suggesting that $MoSe_2$ is more sensitive to N-based gas molecules. Particularly, NO_2 adsorption has the highest adsorption energy, which can help us to understand the mechanism of the $MoSe_2$-FET gas sensor operation upon NO_2 adsorption. The reduced conductance was found for NH_3, NO and NO_2 adsorbed $MoSe_2$, consistent with the high sensitivity of $MoSe_2$ for NH_3 and NO_2 molecules as seen in the recent experiment. In addition, the adsorption sensitivity can be significantly improved by an external electric field. The magnetic moment of adsorbed NO and NO_2 molecules can effectively be modulated by the charge transfer, which is sensitive to the applied electric field. Our results not only explain the recent experiments, but also suggest using $MoSe_2$ as a superior gas sensor.

Acknowledgements

This work is supported in China by the National Natural Science Foundation of China (Nos.11604047, 51672127), the Natural Science Foundation of Jiangsu Province (No. BK20160694), the Priority Academic Program Development of Jiangsu Higher Education Institutions (PAPD), the Fundamental Research Funds for the Central Universities, and the open research fund of Key Laboratory of MEMS of Ministry of Education, Southeast University. AVK acknowledges the Academy of Finland for the support under Project No. 286279. We acknowledge generous grants of computer time from CSC Finland and National Supercomputer Center in Tianjin.

Reference

[1] Abbasi A 2019 *J Inorg. Organomet.* https://doi.org/10.1007/s10904-019-01151-x

[2] Abbasi A 2019 *Physica* E **108** 34

[3] Abbasi A and Sardroodi J J 2017 *New J Chem.* **41** 12569

[4] Abbasi A and Sardroodi J J 2019 *Physica* E **108** 382

[5] Abbasi A 2019 *Synthetic Met.* **247** 26

[6] Abbasi A and Sardroodi J J 2018 *J Appl. Phys.* **124** 165302

[7] Abbasi A and Sardroodi J J 2018 *Appl. Surf. Sci.* **442** 368

[8] Abbasi A and Sardroodi J J 2018 *Comput. Theor. Chem.* **1125** 15

[9] Radisavljevic B, Radenovic A, Brivio J, Giacometti V and Kis A 2011 *Nat. Nanotechnol* **6** 147

[10] Duan X, Wang C, Pan A, Yu R and Duan X 2015 *Chem. Soc. Rev.* **44** 8859

[11] Lembke D, Bertolazzi S and Kis A 2015 *Acc. Chem. Res.* **48** 100

[12] Chhowalla M, Jena D and Zhang H 2016 *Nat. Rev. Mater.* **1** 16052

[13] Manzeli S, Ovchinnikov D, Pasquier D, Yazyev O V and Kis A 2017 *Nat. Rev. Mater.* **2** 17033

[14] Ma Y, Kou L, Li X, Dai Y and Heine T 2016 *Phys. Rev.* B **93** 035442

[15] Schedin F, Geim A K, Morozov S V, Hill E W, Blake P, Katsnelson M I and Novoselov K S 2007 *Nat. Mater.* **6** 652

[16] Mak K F, Lee C, Hone J, Shan J and Heinz T F 2010 *Phys. Rev. Lett.* **105** 136805

[17] Kou L, Frauenheim T and Chen C 2014 *J Phys. Chem. Lett.* **5** 2675

[18] Kou L, Du A, Chen C and Frauenheim T 2014 *Nanoscale* **6** 5156

[19] Perkins F K, Friedman A L, Cobas E, Campbell P M, Jernigan G G and Jonker B T 2013 *Nano Lett.* **13** 668

[20] Abbasi A and Sardroodi J J 2018 *Appl. Surf. Sci.* **436** 27

[21] Abbasi A and Sardroodi J J 2019 *Appl. Surf. Sci.* **469** 781

[22] Zhang W, Huang J K, Chen C H, Chang Y H, Cheng Y J and Li L J 2013 *Adv. Mater.* **25** 3456

[23] He Q, Zeng Z, Yin Z, Li H, Wu S, Huang X and Zhang H 2012 *Small* **8** 2994

[24] Li H *et al* 2012 *Small* **8** 63

[25] Late D J *et al* 2013 *ACS Nano* **7** 4879

[26] Lee K, Gatensby R, McEvoy N, Hallam T and Duesberg G S 2013 *Adv. Mater.* **25** 6699

[27] Yao Y, Tolentino L, Yang Z, Song X, Zhang W, Chen Y and Wong C P 2013 *Adv. Funct. Mater.* **23** 3577

[28] Chen X *et al* 2018 *Adv. Funct. Mater.* **28** 1705153

[29] Lee H, Ahn J, Im S, Kim J and Choi W 2018 *Sci. Rep.* **8** 11545

[30] Zhang S, Nguyen T H, Zhang W, Park Y and Yang W 2017 *Appl. Phys. Lett.* **111** 161603

[31] Late D J, Doneux T and Bougouma M 2014 *Appl. Phys. Lett.* **105** 233103

[32] Baek J *et al* 2017 *Nano Res.* **10** 1861

[33] O'Keeffe J, Wei C and Cho K 2002 *Appl. Phys. Lett.* **80** 676

[34] Li Y, Rotkin S V and Ravaioli U 2003 *Nano Lett.* **3** 183

[35] Ao Z M, Zheng W T and Jiang Q 2008 *Nanotechnology* **19** 275710

[36] Liang X Y, Ding N, Ng S P and Wu C M L 2017 *Appl. Surf. Sci.* **411** 11

[37] Yue Q, Shao Z, Chang S and Li J 2013 *Nanoscale Res. Lett.* **8** 425

[38] Li T T, He C and Zhang W X 2018 *Appl. Surf. Sci.* **427** 388

[39] Kresse G and Furthmüller J 1996 *Phys. Rev.* B **54** 11169

[40] Kresse G and Furthmüller J 1996 *Comp. Mater. Sci.* **6** 15

[41] Perdew J P, Burke K and Ernzerhof M 1996 *Phys. Rev. Lett.* **77** 3865

[42] Blöchl P E 1994 *Phys. Rev.* B **50** 17953

[43] Kresse G and Joubert D 1999 *Phys. Rev.* B **59** 175851

[44] Grimme S 2006 *J Comp. Chem.* **27** 1787

[45] Bučko T Hafner J Lebègue S and Ángyán J G 2010 *J Phys. Chem.* A **114** 11814

[46] Henkelman G, Arnaldsson A and Jónsson H 2006 A *Comp. Mater. Sci.* **36** 354

[47] Brandbyge M, Mozos J L, Ordejón P, Taylor J and Stokbro, K 2002 *Phys. Rev.* B **65** 165401.

[48] Hu X, Kou L and Sun L 2016 *Sci. Rep.* **6** 31122

[49] Hu X, Wang Y, Shen X, Krasheninnikov A V, Sun L and Chen Z 2018 *2D Mater.* **5** 031012

[50] Cho B *et al* 2015 *Sci. Rep.* **5** 8052

[51] Leenaerts O, Partoens B and Peeters F M 2008 *Phys. Rev.* B **77** 125416